Secondary focusable and uniform convergence microprism in concentrating photovoltaic module

Limin Guo [1, 2], Zhiyong Wang [2], Youqiang Liu [2], Songxuan Chen [1], Ying Zhang [1], June Liu [1, *]

[1] China ENFI Engineering Corporation, Beijing, China
[2] Institute of Laser Engineering, Beijing University of Technology, Beijing, China

Abstract. Low tracking accuracy of trackers, structure vibration by winds, and lens deformation by temperature lead to non-vertical incident irradiation of Fresnel lens, which necessitates a secondary concentrator in actual engineering application of concentrating photovoltaic module. In this study, a secondary focusable and uniform convergence microprism is added between Fresnel lens and solar cell to improve concentrating efficiency and focal spot energy uniformity. The 3D model of microprism is established by SolidWorks, and important parameters are optimized using Zemax. Results showed that combination of Fresnel lens and focusable and uniform convergence microprism achieves the highest power when upper spherical diameter of secondary microprism measures 18 mm, included angle in opposite side facets equals 116°, spherical height removed from the top is 0.1 mm, and side length of bottom reaches 2.15 mm. The highest power of solar cell surface can reach 2.4932 W, representing a 32.9% improvement; focal spot energy uniformity is 0.71; and module height with secondary microprism measures 88 mm, which reduces by 5.5 mm without secondary microprism. Experimental results show that concentrating static test generation efficiency of a 400-times concentrating module system reaches 34.9%, acceptance angle measures ±1.18°, efficiency loss of module is less than 1.23% when temperature changes from −20°C to 20°C and from 20°C to 50°C, and 400-times module maximum output power totals 142.3 W.

1. Introduction

High concentrating photovoltaic (HCPV) systems rely on large Fresnel lens, which must be precisely oriented in the direction of the sun to maintain high concentration ratio [1]. When tracking systems exhibit certain accuracy, then HCPV system features high acceptance angle and low power loss. Many photovoltaic (PV) plants are distributed in subtropic and temperate climate zones, such as Hami, Golmud, and Nyemo in China. These light intensity regions usually show large temperature differences between day and night and during summer and winter. When temperature changes, deformations of Fresnel lens lead to changes in refractive index; such changes offset focus on battery-receiving surface and result in higher energy loss. Fresnel lens exhibit poor acceptance angle and temperature adaptability; therefore, a suitable secondary optical component is designed to improve concentrating performance.

Several institutes worked on new types of secondary concentrators and their application in concentrating photovoltaic (CPV) modules [2-3]. João Mendes-Lopes et al. improved secondary concentrators, which are divided into nine centrosymmetric areas, and their simulation results showed high irradiance uniformity of focal spots [4]. Tian Gu et al. introduced the microsystem-enabled PV using non-imaging micro-concentrators and III-V solar cells, which combined toroidal primary lens and reflective cone secondary concentrator to enhance light collection and illumination onto microscale solar cells and to achieve an acceptance angle product of more than 1° [5-6]. Zeng Fei et al. designed a total internal reflection-refraction solar concentrator combined with a homogenizer. In this design, the highest irradiance intensity is less than twice of average irradiance intensity on cell surface, and acceptance angle measures 1.5°[7].

Although previously discussed secondary concentrator designs show high optical performances, difficulty arises from their machining and assembly. This problem increases cost of CPV systems and restrict further development of this technology. This study presents a focusable and energy-uniform secondary microprism, which features an inverted truncated rectangular pyramid at the bottom and spherical and flat surface on top. With its simple structure, good work ability, and stable performance, this design shows potential in practical HCPV application.

2. Concentrating results without secondary microprism

Area of solar cell totals 2.5×2.5 mm^2, area of Fresnel lens measures 50×50 mm^2, concentration ratio is set to 400, and focus of Fresnel lens is set to 94 mm. Fresnel lens substrate is an ultra-white glass with thickness measuring

* Corresponding author: 277040689@qq.com

3.2 mm. Lens material is silicon with thickness of 1 mm. Room temperature measures 20°C.

The 3D model of Fresnel lens is established by the SolidWorks software, and Zemax optical simulation software is introduced to perform computer simulation. Custom light source in Zemax is used, source parameters are set based on AM1.5D standard spectral correlation parameters, and lens material parameters are set based on silicon parameters. Solar radiation is set to 1,000 W/m^2, which is the standard intensity. When light is normally incident on the surface of Fresnel lens, power of focusing spot is the highest, i.e., 1.8764 W, as shown in Figure 1 and 2. Simulation results show that concentrating efficiency of Fresnel lens totals 75%, focal spot energy uniformity is 0.59, and acceptance angle measures ± 0.64°. At room temperature of 20°C, decrease in concentrating efficiency of Fresnel lens exceeds 15.7% when temperature changes from -20°C to 20°C and from 20°C to 50°C. Maximum output power of the 400-times module with Fresnel lens measures 111.8 W. Thus, a suitable secondary optical component should be designed to improve concentrating performance.

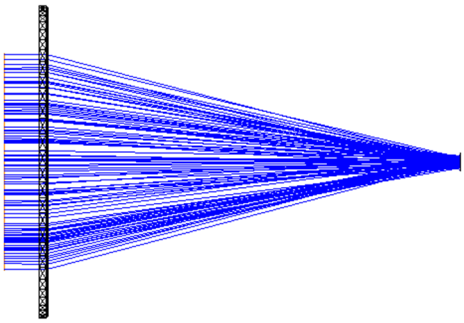

Figure 1. Concentrating effect with Fresnel lens

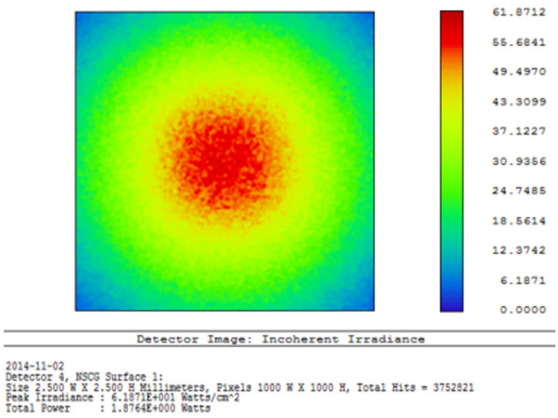

Figure 2. Energy distribution of focal spot on solar cell surface

3. Principle of secondary focusable and uniform convergence microprism

Secondary focusable and uniform convergence microprism is inserted between Fresnel lens and solar cell to improve concentrating performance. The truncated rectangular pyramid below the secondary microprism concentrates light, with the bottom rectangular facet linking the solar cell and its dimensions matching that of cell. The other four side facets work as total reflection plane, and included angle of opposite side facets is set as α. Top spherical and flat surface of secondary microprism is used as incident plane, in which the spherical part focuses solar rays, and the flat part ensures energy uniformity of solar cell surface. Fig. 3 depicts the optical path of secondary microprism, and Fig. 4 displays the 3D model of secondary microprism. Incident light is allowed to pass no more than one total reflection in the secondary microprism before it is absorbed by cell to reduce incident energy loss. In this study, air refractive index is set as n_1, and refractive index of secondary microprism is set as n_2.

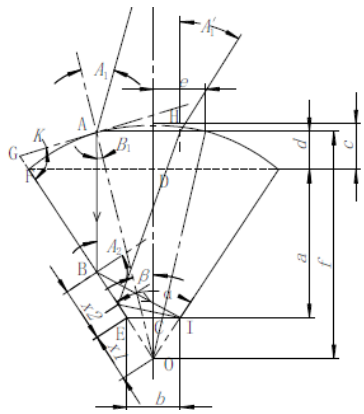

Figure 3. Optical path of secondary microprism

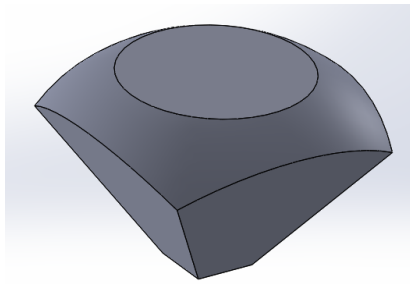

Figure 4. 3D model of secondary microprism

When light is incident on spherical surface and based on refraction and total reflection laws, this study deduces the following:

$$n_1 \sin A_1 = n_2 \sin B_1 \tag{1}$$

$$A_2 \geq \arcsin \frac{n_1}{n_2} \tag{2}$$

With Δ ABO, Δ EIO, and Δ BEI and based on geometrical relationship and law of sines, this study deduces that:

$$\frac{R}{\sin(\frac{\pi}{2} + A_2)} = \frac{x_1 + x_2}{\sin B_1} \tag{3}$$

$$\frac{b}{\sin \alpha} = \frac{x_1}{\sin(\frac{\pi - \alpha}{2})} \tag{4}$$

$$\frac{b}{\sin(\frac{\pi}{2}-A_2)}=\frac{x_2}{\sin(A_2-\frac{\alpha}{2})} \tag{5}$$

From Formulas (1) to (5), the following expression can be derived:

$$A_1 \le \arcsin\frac{n_2 b\cos(\arcsin\frac{n_1}{n_2}-\alpha)}{2n_1 R\sin\frac{\alpha}{2}} \tag{6}$$

When light is incident on flat surface and based on reference [8-11], this study deduces that:

$$\pi-\alpha \ge \arcsin\frac{n_1}{n_2}\pi-\alpha \ge \arcsin\frac{n_1}{n_2}+\arcsin(\frac{n_1}{n_2}\sin A_1') \tag{7}$$

Then, incident angle should meet the following condition:

$$A_1' \le \arcsin(\frac{n_2}{n_1}\sin\alpha\sqrt{1-\frac{n_1^2}{n_2^2}}+\cos\alpha) \tag{8}$$

Formulas (6) and (8) show required conditions of secondary focusable and uniform convergence microprism.

Fresnel lens can be simplified into a thin lens, and the top spherical surface of secondary microprism focusing the lights can be considered a planoconvex lens. Thus, the distance H between Fresnel lens and secondary microprism should be designed. Based on the formula of combined focal length, the following expression can be derived:

$$f'=\frac{f_1' f_2'}{f_1'+f_2'-H}=\frac{1.8L\times\frac{R}{n_{K9}(\lambda)-1}}{1.8L+\frac{R}{n_{K9}(\lambda)-1}-H} \tag{9}$$

$$\begin{cases} l_H'=-f'\frac{H}{f_1'}=-\frac{1.8L\times\frac{R}{n_{K9}(\lambda)-1}\times H}{(1.8L+\frac{R}{n_{K9}(\lambda)-1}-H)\times 1.8L} \\ l_H=f\frac{H}{f_2}=\frac{1.8L\times\frac{R}{n_{K9}(\lambda)-1}\times H}{(1.8L+\frac{R}{n_{K9}(\lambda)-1}-H)\times\frac{R}{n_{K9}(\lambda)-1}} \end{cases} \tag{10}$$

According to Formulas (9) and (10), the distance H between Fresnel lens and secondary microprism can be optimized.

4. Optimization design of secondary focusable and uniform convergence microprism in the 400-times module

Given the machining precision and cell dimension, in this study, parameter b is set to 2.15 mm. Zemax is used to optimized included angle α in opposite side facets, spherical diameter 2R, and spherical height g removed from the top. The material of this secondary mIcroprism is K9 or Bk7.

Assuming that the initial value of secondary microprism spherical diameter 2*R* measures 16 mm, and spherical height *g* removed from the top totals 0 mm, then included angle *α* in opposite side facets varies from 100° to 140°. Considering every 1° in this interval range and simulating them in Zemax software combined with other determined parameters, power curve received by solar cell is constructed and shown in Fig. 5. According to simulation results, maximum power received by the solar cell measures 2.4876 W when *α* equals 116°.

Supposing that the initial value of included angle *α* in opposite side facets totals 116°, and spherical height *g* removed from the top measures 0 mm, then spherical diameter 2*R* varies from 15 mm to 27 mm. Obtaining every 0.5 mm interval in this range and simulating them in Zemax software combined with other determined parameters, energy curve received by the solar cells is constructed and shown in Fig. 6. Based on simulation results, maximum power received by the solar cell reaches 2.4907 W when 2*R* is set to 18 mm.

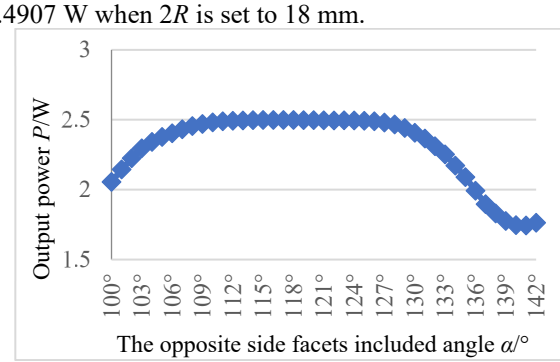

Figure 5. The α-optimized result with output power

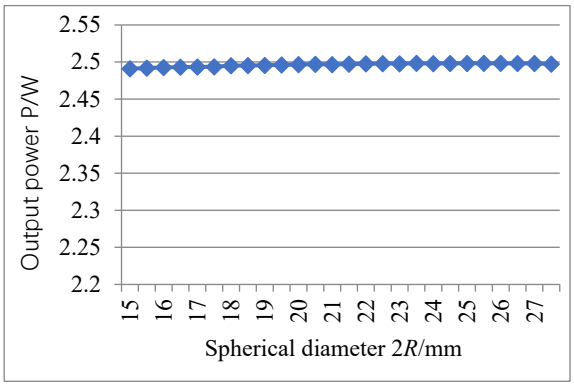

Figure 6. 2R-optimized result with output power

Supposing that initial value of included angle *α* in opposite side facets totals 116°, and spherical diameter *2R* measures 18 mm, then spherical height *g* removed from the top ranges from 0 mm to 1 mm. Considering every 0.1 mm interval in this range and simulating them in Zemax software combined with other determined parameters, energy curve received by the solar cell is constructed, as shown in Fig. 7, and focal spot energy uniformity curve is determined, as indicated in Fig. 8. According to simulation results, maximum power received by the solar cell totals 2.4911 W, and focal spot energy uniformity measures 0.71 when g is set to 0.2 mm.

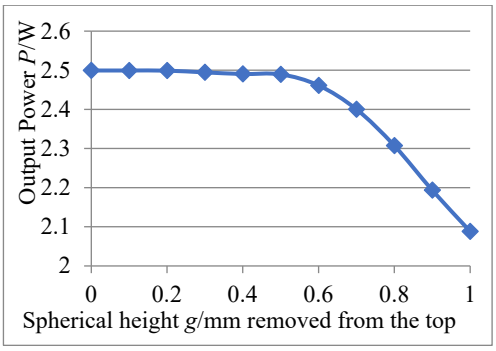

Figure 7. The g-optimized result with output power

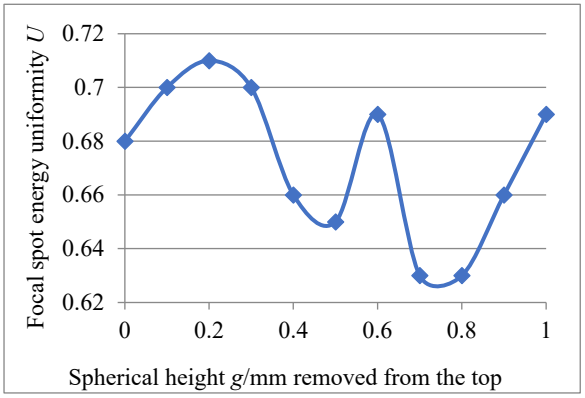

Figure 8. The g-optimized Result optimized with focal spot energy uniformity

5. Concentrating performance analysis of the 400-times module with secondary focusable and uniform convergence microprism

When parameters of secondary microprism are determined, the distance *H* between Fresnel lens and secondary microprism can be optimized using Zemax. Height *H* is changed from 80 mm to 96 mm. Considering every 2 mm interval in this range and simulating them in Zemax software combined with other determined parameters, power values received by the solar cell are determined and listed in Table 1. Based on simulation results, maximum power received by the solar cell totals 2.4932 W when *H* is set to 88 mm, which is reduced by 6 mm without the secondary microprism. Figure 9 and 10 display results of concentrating performance.

Figure 9 and 10 show that concentrating efficiency reaches 99.72%, indicating a 24.72% increase, and focal spot energy uniformity totals 0.71, presenting a 20.3% increase, without the secondary microprism. Notably, the secondary microprism hardly affects concentrating performance of the module.

Table 1. Energy received by solar cell combined with secondary microprisms of different heights

H (mm)	80	82	84	86	88
Power (W)	2.4866	2.4907	2.4913	2.4923	2.4932
H (mm)	90	92	94	96	98
Power (W)	2.4924	2.4916	2.4911	2.4874	2.4821

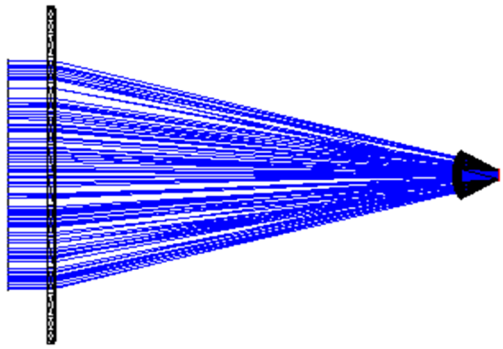

Figure 9. Concentrating effect with Fresnel lens and secondary microprism

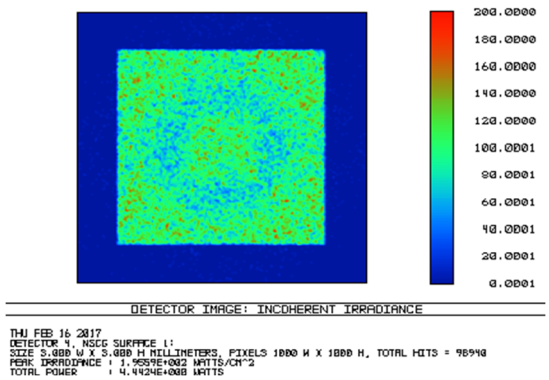

Figure 10. Energy distribution of focal spot on solar cell surface with Fresnel lens and secondary microprism

When light is normally incident on the surface of Fresnel lens, energy of focusing spot is the highest. With increasing incident light angle, some lights cannot focus on battery-receiving surface. Thus, beam energy decreases gradually. Fig. 11 shows the relationship between incident light angle and focal spot energy. When tilt angle of incident light in one direction approximates 1.18°, energy of receiving surface of battery decreases to 2.2501 W. Approximately 90% of the battery receives energy when light is normally incident. Thus, acceptance angle measures ±1.18° during simulation. Fig. 12 shows energy distribution of the focal spot on solar cell surface with incident light angle of 1.18°.

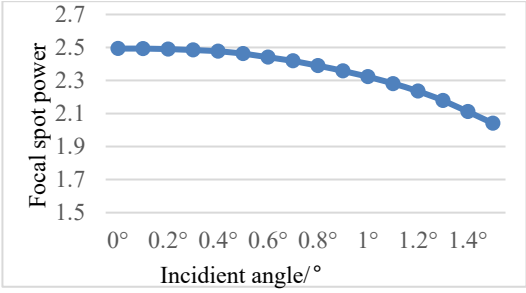

Figure 11. Dependence of focal spot power on incident angle

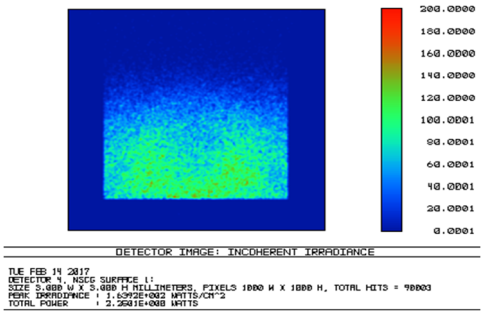

Figure 12. Energy distribution with incident angle of 1.18°

Temperature change leads to changes in teeth parameters of Fresnel lens and refractive index of silicon. Parameter changes in Fresnel lens are simulated using Zemax. Figure 13 and 14 show energy distribution of focal spots on the solar cell surface at temperatures of -20 °C and 50 °C, respectively.

Figure 9 and 10 show that energy of receiving surface of battery measures 2.462 W when temperature is -20 °C and 2.464 W when temperature is 50 °C, and efficiency loss of module measures less than 2.5% when temperature changes from -20 °C to 20 °C and from 20 °C to 50 °C.

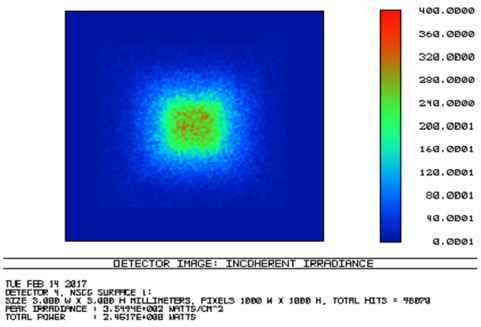

Figure 13. Energy distribution at −20°C

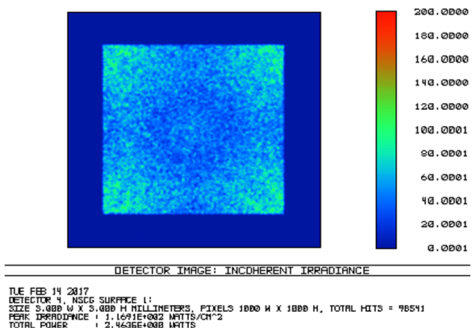

Figure 14. Energy distribution at 50°C

6. Experiment on the 400-times module with secondary focusable and uniform convergence microprism

Focusable and uniform convergence secondary microprism is constructed according to the following simulation parameters: α = 116°, 2R = 18 mm, b = 2.15 mm, g = 0.2 mm, as illustrated in Fig. 15. Fig. 16 shows experimental 400-times module, with a distance H of 88 mm. Fresnel lens features an optical efficiency of 75%. The solar cell is a 40% efficient GaAs-based triple-junction solar cell.

I–V curves of experimental module are tested using a sun simulator with 850 W/m^2 and parallel light intensity under two kinds of conditions, namely, vertical incidence and oblique incidence, at room temperature of 20 °C. Fig. 17 displays I–V curves of vertical incidence at room temperature of 20 °C and with maximum output power of 142.3W. The sun simulator can test I–V curves depending on different incident angles. Simulation results show that when temperature increases or decreases, actual focal length of concentrating module lengthens or shortens and changes by 1 mm for every 10 °C increment. Therefore, experiments on temperature effect are conducted by changing module height. Output power curve depends on different heights of the module, as shown in Fig. 18. When module height increases by 4 mm, output power totals 139.1 W, representing a 2.3% decrease. When module height decreases by 3 mm, output power reaches 138.7W, indicating a 2.6% decrease. These findings coincide with simulation results.

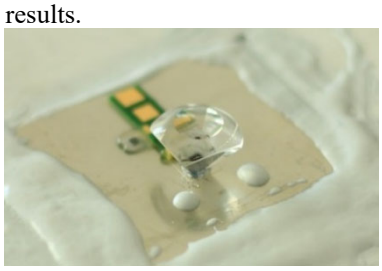

Figure 15. Energy distribution at -20°C

Figure 16. Energy distribution at 50°C

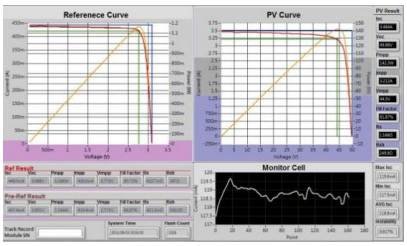

Figure. 17. I–V test curve with vertical incidence

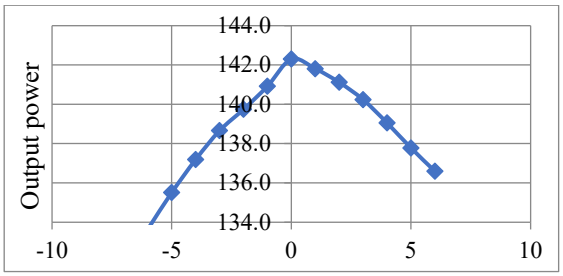

Figure 18. Relationship between module height change and output power

7. Conclusion

In this study, a focusable and uniform convergence secondary microprism is designed to improve performance of CPV module. Geometric parameters are optimized through 3D modeling and Zemax simulation. Focusable and uniform convergence secondary microprism is manufactured according to simulation parameters, and experimental 400-times module is tested to verify simulation results. Experimental observations agree with simulation results.

Results show that combination of Fresnel lens and focusable and uniform convergence microprism features the highest energy when upper spherical diameter of secondary microprism measures 18 mm, included angle of opposite side facets totals 116°, side length of bottom reaches 2.15 mm, and spherical height g removed from the top is 0.2 mm. Concentrating efficiency of the 400× concentrating module system reaches 88.67%, acceptance angle totals ±1.2°, maximum output power of 400× module measures 142.3 W, and efficiency loss of the module is less than 2.6% when temperature changes from −20 °C to 20 °C and from 20 °C to 50 °C. Compared with the case without secondary microprism, output power increases by 27.3%, acceptance angle increases by 87.5%, and efficiency loss of module decreases by 83.4%, indicating a significant improvement in generation performance of CPV module. This focusable and uniform convergence secondary microprism has been widely applied in Delingha 50MW power generation project.

References

1. W.T. Xie, Y.J. Dai, R.Z. Wang, and K. Sumathy, Concentrated solar energy applications using Fresnel lenses: A review, Renew, Sust. Energ., 15 (2011) 2588–2606.
2. B. Pablo, C.M. Juan, Z. Pablo, M. Rubén, C.Aleksandra, B. Marina, C. Julio, and H. Maikel, High performance Fresnel-based photovoltaic concentrator, Opt. Express, 18, S1 (2010) 25-40.
3. J.C. Miñano, P. Benítez, P. Zamora, M. Buljan, R. Mohedano, and A.Santamaría, Free-form optics for Fresnel-lens-based photovoltaic concentrators, Opt. Express, 21, S3 (2013) 494-502.
4. M.L. João, P. Benítez, P. Zamora, J.C. Miñano, and P.Adam, 9-fold Fresnel–Köhler concentrator with Fresnel lens of variable focal point, Opt. Express, 22, S4 (2014) 1153-1163.
5. B. Jared, M. Saavedra, B. Anderson, R. Goeke, W. Sweatt, G. Nielson, M. Okandan, B. Elisberg, D. Snively, J. Duncan, T. Gu, G. Agrawal, and M. Haney, Micro-concentrators for a microsystems-enabled photovoltaic system , Opt. Express, 22 (2014) 521-527 .
6. T. Gu, W.C. Sweatt, G. Agrawal, B.H. Jared, B.J. Anderson, R.S. Goeke, B. Elisberg, S.M. Paap, J.L. Cruz-Campa, V. Gupta, M. Okandan, G.N. Nielson, and M.W. Haney, Decentralized nonimaging micro-optical concentrator, Efficient Design for Illumination and Solar Concentration XI, Proc. of SPIE, 2014, 91910G.
7. F. Zeng, H.T. Li, and Z.B. Hao, High-concentration solar concentrator with uniform irradiation, Acta Energiae Solaris Sinica, 33, S2 (2012) 338-342 .
8. G.H. Yang, B.Z. Chen, Y.Q. Liu, L.M. Guo, Y. Shun, Z.Y. Wang, Optimized Design and Research of Secondary Microprism for Dense array Type Concentrating Photovoltaic Module, Applied Optics and Photonics, 2015, 967603.
9. R. Huang, L.M. Guo, Y.Q. Liu, C.C. Wang, M. Zhao, X.N. Zhang, H.M. Zhang, Z.Y. Wang, and Y.H. Cao, Research and Design of High Power Concentrator Module System, Chinese Journal of Luminescence, 39 S7 (2018) 974-982 .
10. L.M. Guo, Y.Q. Liu, G.M. Zhao, and Z.Y. Wang, Design and research of focusable secondary microprism in concentrating photovoltaic module, Proceeding of CPV-13 conference, Ottawa, AIP conference Proceeding, 2017, 1881.
11. L.M. Guo, Y.Q. Liu, Y.T. Qiu, and Z.Y. Wang, Design and research on Fresnel lens of combination of equal-width and equal-height of grooves. IOP Conference Series: Earth and Envionmental Science, 2017, 69:012177.